Why Galaxies Care About AGB Stars: A Continuing Challenge through Cosmic Time
Proceedings IAU Symposium No. 343, 2019
F. Kerschbaum, M. Groenewegen & H. Olofsson, eds.

doi:10.1017/S1743921318005446

Newly discovered Planetary Nebulae population in Andromeda (M31): PN Luminosity function and implications for the late stages of stellar evolution

Souradeep Bhattacharya[1]†, Magda Arnaboldi[1], Johanna Hartke[1], Ortwin Gerhard[2], Valentin Comte[1,3], Alan McConnachie[4] and William E. Harris[5]

[1]European Southern Observatory, Karl-Schwarzschild-Str. 2, 85748 Garching, Germany
email: sbhattac@eso.org

[2]Max-Planck-Institut für Extraterrestrische Physik, Giessenbachstrasse, 85748 Garching, Germany

[3]Aix Marseille Université, CNRS, LAM Laboratoire d'Astrophysique de Marseille, 38 rue F. Joliot-Curie, 13388 Marseille, France

[4]NRC Herzberg Institute of Astrophysics, 5071 West Saanich Road, Victoria, BC V9E 2E7, Canada

[5]Department of Physics & Astronomy, McMaster University, Hamilton, ON L8S 4M1, Canada

Abstract. Stars with masses between ~ 0.7 and 8 $M_{\odot}$ end their lives as Planetary Nebulae (PNe). With the MegaCam at CFHT, we have carried out a survey of the central 16 sq. degrees of Andromeda (M31) reaching the outer disk and halo, using a narrow-band [OIII]5007 and a broad-band g filter. This survey extends previous PN samples both in uniform area coverage and depth. We identify ∼4000 PNe in M31, of which ∼3000 are new discoveries. We detect PNe down to ∼6 mag below the bright cut-off of the PN luminosity function (PNLF), ∼2 mag deeper than in previous works. We detect a steep rise in the number of PNe at ∼4.5 mag fainter than the bright cut-off. It persists as we go radially outwards and is steeper than that seen in the Magellanic clouds. We explore possible reasons for this rise, which give insights into the stellar population of M31.

Keywords. galaxies: individual (M31), planetary nebulae: general

---

1. Introduction

Having recently left the AGB, PNe are observed to be the glowing shells of gas and dust around stars that are evolving towards the white dwarf stage. The short timescales between the AGB and PN phases imply that the distribution and kinematics of PNe are expected to be drawn from the line-of-sight velocity (LOSV) distribution of their parent population. Due to their relatively strong [OIII] 5007 Å emission and no continuum

† Based on observations obtained with MegaCam, a joint project of CFHT and CEA/DAPNIA, at the Canada-France-Hawaii Telescope (CFHT) which is operated by the National Research Council (NRC) of Canada, the Institut National des Science de l'Univers of the Centre National de la Recherche Scientifique (CNRS) of France, and the University of Hawaii. The observations at the CFHT were performed with care and respect from the summit of Maunakea which is a significant cultural and historic site.

emission, PNe can be easily identified in external galaxies as point sources and studying them as a population provides insight into galactic structure and evolution.

From the integrated [OIII] 5007 Å flux, the m_{5007} magnitude is measured. For an extragalactic PN population, we can then measure its luminosity function (hereafter PNLF) that is observed to have an absolute bright cut-off (Ciardullo *et al.* 1989; C89) mostly invariant with metallicity and age of the parent stellar population, and galaxy type. It is thus used as a secondary distance indicator for determining galactic distances out to ∼20 Mpc. The faint-end of the PNLF can be described by an exponential function (Jacoby 1980) expected from slowly evolving central stars embedded in rapidly expanding, optically thin nebulae (Henize & Westerlund 1963). The PNLF slope has been shown to be correlated with the star formation history of the parent stellar population, with steeper slopes associated with older stellar populations and flatter slopes with younger populations (Ciardullo *et al.* 2004; Longobardi *et al.* 2013).

M31 is the closest giant spiral disk to our Milky Way (MW) at a distance of ∼ 780 kpc. The Pan-Andromeda Archaeological Survey (PAndAS; McConnachie *et al.* 2009) map of the resolved stellar population number counts showed the wealth of substructures, which are residues of past accretion events, present in the M31 halo (see Ferguson & Mackey 2016). Merrett *et al.* (2006; M06) uniformly surveyed the disk and bulge of M31 down to ∼ 3.5 - 4 mag below the bright cut-off. A uniform deep survey of PNe in the halo of M31 and the inner-halo substructures is necessary not only to unambiguously trace the metal-poor halo and inner halo substructures, but also to probe the variation in the PNLF further out from the disk. This will allow us to corroborate the invariant nature of its bright cut-off and observe the effects on its faint end.

2. CFHT MegaCam M31 PNe survey

We survey the inner 16 sq. deg. of M31 (∼20-30 kpc from its center), covering the disk and the inner halo including its substructures. The observations were carried out with the MegaCam wide-field imager (Boulade *et al.* 2003) mounted on the 3.6-m Canada France Hawaii Telescope (CFHT). M31 is observed through a narrow-band [OIII] filter ($\lambda_c =$ 5007 Å, $\Delta\lambda = 102$ Å, on-band) and a broad-band g filter ($\lambda_c = 4750$ Å, $\Delta\lambda = 1540$ Å, off-band). The fields are shown in Fig 1. We used SExtractor (Bertin & Arnouts 1996), a source detection algorithm that detects and measures flux from point-like and extended sources, to detect and carry out photometry of the sources on the images.

Extragalactic PNe can be identified as point-like objects detected in the on-band images but not in the off-band images. To detect PNe, we used the automatic selection procedure developed and validated in Arnaboldi *et al.* (2002, 2003) and later adapted to larger surveys by Longobardi *et al.* (2013) and Hartke *et al.* (2017). We simulate synthetic point-like populations for each field following a PNLF described in C89 onto the on- and off-band images to determine the limiting magnitude of our sample for each field, remove contamination from continuum sources, and correct for incompleteness effects. We identify over 4000 PNe in M31, of which only ∼ 1100 were previously identified by M06. Our survey is uniformly complete down to 5.5 mag below the bright cut-off, reaching 6.4 mag below the bright cut-off in the deepest field. Details of the data reduction and PNe identification are described in Bhattacharya *et al.* (2018; in preparation; Bh+18)

We tested the astrometric quality of our PNe survey, and checked the contamination from HII regions which affected the M06 PNe sample (Sanders *et al.* 2012; Veyette *et al.* 2014) and other sources, by identifying PNe counterparts in the *Hubble Space Telescope* data available from the Panchromatic Hubble Andromeda Treasury (Dalcanton *et al.* 2012). The PHAT survey covers ∼ 1/3 of the star-forming disk of M31, using HSTs imaging cameras (WFC3/IR, WFC3/UVIS, and ACS/WFC cameras) in six bands. We

https://doi.org/10.1017/S1743921318005446 Published online by Cambridge University Press

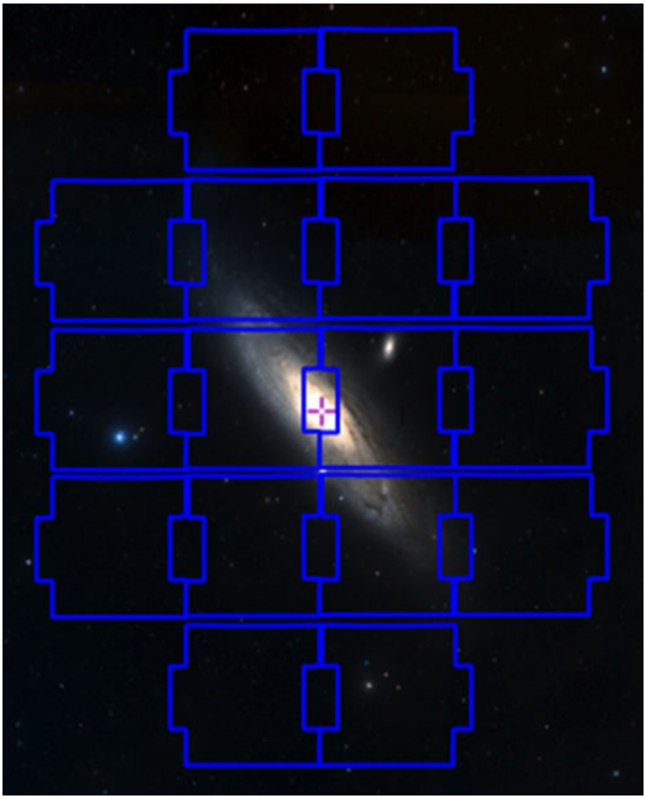

Figure 1. The fields observed with CFHT MegaCam shown in blue. The background image is from SDSS obtained using the Aladin Sky Atlas (Bonnarel *et al.* 2000).

find that of the PNe with counterparts in the PHAT sample, only $\sim 3\%$ may be stellar contamination but none of them were resolved HII regions, owing to the excellent resolution we have with MegaCam (Bh+18 for details).

3. Planetary Nebula Luminosity Function

Fig 2 shows the PNLF for PNe identified in one of the fields in our survey. The PNLF measured from the extended and deep PN catalogue and the extensive catalogue validation are presented in Bh+18. While the bright cut-off and the fitted slope are found to be consistent with those determined by M06 and C89, there is a significant rise in the faint end of the PNLF which remains invariant as we go radially outwards. This indicates that the rise is ubiquitous throughout the surveyed area and not due to crowding or other observational effects. It is steeper than the PNLF observed for the Magellanic clouds (LMC- Reid & Parker 2010; SMC- Jacoby & De Marco 2002). The faint-end rise of the PNLF is also present in the PHAT subsample. This subsample is further investigated for symbiotic stars mimicking PNe in our survey. With HST colours, we can rule out this hypothesis.

The rise in the faint-end of the PNLF appears to be physical and associated with the PN population of M31. It thus reflects the properties of its parent stellar population. The faint-end rise in the PNLF might be due to multiple populations of different ages in M31 that populate different magnitude intervals of the PNLF. Another possible explanation for the rise in the faint-end of the PNLF could be a change in opacity of the nebula of the

https://doi.org/10.1017/S1743921318005446 Published online by Cambridge University Press

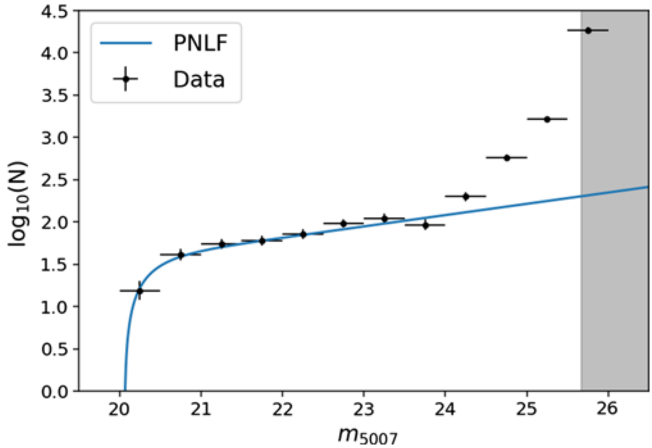

Figure 2. The completeness-corrected PNLF is shown for a single field of our survey, fitted by the C89 analytical LF (in blue). The region beyond the 50% completeness limit is shown in grey.

PNe, previously considered to describe the dip in the PNLF seen in the SMC (Jacoby & De Marco 2002) and also seen in the models by Gisecki *et al.* (2018).

4. Future prospects

We are planning to extend our imaging survey to ~ 50 kpc from the center of M31 to investigate the nature of the PNLF further out in the halo. We are also planning a spectroscopic follow-up of a complete subsample of the M31 PNe with Hectospec at the MMT (Fabricant *et al.* 2005) to obtain their LOSV to kinematically disentangle the M31 spheroid from the substructures and to identify the circumstellar extinction for the brightest PNe, ~ 2 mag below the bright cut-off.

Acknowledgements

SB would like to thank the organizers of the IAU Symposium S343 for the opportunity to present a contributed talk. SB and JH acknowledge support from the IMPRS on Astrophysics at the LMU Munich.

References

Arnaboldi, M., Aguerri, J. A. L., Napolitano, N. R., *et al.* 2002, *AJ*, 123, 760
Arnaboldi, M., Freeman, K. C., Okamura, S., *et al.* 2003, *AJ*, 125, 514
Bertin, E., & Arnouts, S. 1996, *A&AS*, 117, 393
Bonnarel F., Fernique P., Bienaym O., *et al.*, 2000, *A&AS*, 143, 33
Boulade, O., Charlot, X., Abbon, P., *et al.* 2003, *in Instrument Design and Performance for Optical/Infrared Ground-based Telescopes, ed. M. Iye, & A. F. M. Moorwood, Proc. SPIE*, 4841, 72
Ciardullo, R., Jacoby, G. H., Ford, H. C., & Neill, J. D. 1989, *ApJ*, 339, 53 [C89]
Ciardullo, R., Durrell, P. R., Laychak, M. B., *et al.* 2004, *ApJ*, 614, 167
Dalcanton, J. J., Williams, B. F., Lang, D., *et al.* 2012, *ApJS*, 200, 18
Fabricant, D., Fata, R., Roll, J., *et al.* 2005, *PASP*, 117, 1411
Ferguson A. M. N., Mackey A. D., 2016, *Astrophysics and Space Science Library, Vol. 420, Tidal Streams in the Local Group and Beyond. Springer International Publishing, Switzerland*, p. 191
Gesicki, K., Zijlstra, A. A., & Miller Bertolami, M. M. 2018, *Nature Astronomy*, 2, 580
Hartke, J., Arnaboldi, M., Longobardi, A., *et al.* 2017, *A&A*, 603, A104

https://doi.org/10.1017/S1743921318005446 Published online by Cambridge University Press

Henize, K. G., & Westerlund, B. E. 1963, *ApJ*, 137, 747
Jacoby, G.H. 1980, *ApJS*, 42, 1
Jacoby, G. H. & De Marco, O., 2002, *AJ*, 123, 269
Jones, D. & Boffin, H. M. J. 2017, *Nature Astronomy*, 1, 0117
Longobardi, A., Arnaboldi, M., Gerhard, O., *et al.* 2013, *A&A*, 558, A42
McConnachie A. W. *et al.*, 2009, *Nature*, 461, 66
Merrett, H. R., Merrifield, M. R., Douglas, N. G., *et al.* 2006, *MNRAS*, 369, 120 [M06]
Reid, W. A. & Parker, Q. A., 2010, *MNRAS*, 405, 1349
Sanders, N. E., Caldwell, N., McDowell, J. *et al.* 2012, *ApJ*, 758, 133
Veyette, M. J., Williams, B. F., Dalcanton, J. J., *et al.* 2014, *ApJ*, 792, 121

https://doi.org/10.1017/S1743921318005446 Published online by Cambridge University Press